Effect of CuO on Dielectric Properties of Perovskite Titanate and Hexagonal Manganite

---

A thesis submitted in partial fulfilment

FOR THE DEGREE OF MASTER OF SCIENCE IN PHYSICS

Under Academic Autonomy

NATIONAL INSTITUTE OF TECHNOLOGY, ROURKELA

By

Hari sankar mohanty

Roll no:-411PH2102

Under the guidance of

Prof. S. Panigrahi

DEPARTMENT OF PHYSICS

NATIONAL INSTITUTE OF TECHNOLOGY,

ROURKELA-769008, 2012-2013

NATIONAL INSTITUTE OF TECHNOLOGY ROURKELA

CERTIFICATE

This is to certify that the thesis entitled, **"Effect of CuO on Dielectric properties of perovskite Titanate and Hexagonal Manganite"** submitted by Hari sankar mohanty in partial fulfillments for the requirements for the award of Master of Science Degree in Physics Department at National Institute of Technology, Rourkela is an authentic work carried out by him under my supervision and guidance.

To the best of my knowledge, the matter embodied in the project has not been submitted to any other University/Institute for the award of any Degree or Diploma.

Rourkela
Date: 8.5.13

Prof. S. Panigrahi
Dept. of Physics
National Institute of Technology
Rourkela-769008

ACKNOWLEDGEMENT

With deep regards and profound respect, I avail this opportunity to express my deep sense of gratitude and indebtedness to Prof.S.Panigrahi, Department of Physics, National Institute of Technology Rourkela, for introducing the present project topic and for his inspiring guidance, constructive criticism and valuable suggestion throughout the project work. I most gratefully acknowledge his constant encouragement and help in different ways to complete this project successfully. I would like to acknowledge my deep sense of gratitude to Prof.Viswakarma, Prof. Pawan Kumar and Prof. Dillip kumar Pradhan Department of Physics, National Institute of Technology Rourkela, for allowing me to use the facilities in the laboratory. I wish to thank all the faculty members & staffs of Department of Physics for their support and help during the project. It gives me great pleasure to express my heartfelt gratitude to the laboratorymate, Mr Rakesh Muduli, Mr.Ranjit Pattanayak,Subrat kar, Ranjit panda, Achyut Biswal, Ms. Priyambada nayak who have made it so easy to work in the laboratory by providing me with a outmost friendly humorus and a micable atmosphere to workin. Last but not the least; I would like to express my gratefulness to my parents for their endless support, without which I could not complete my project work. I would also like to thanks to my friends and all the Ph.D students in our physics department for their valuable help.

Rourkela HARI SANKAR MOHANTY

Date: 8.5.13

CONTENTS

Abstract

Giant dielectric material CuO is chosen suitably to make composite with insulating $SrTiO_3$ and semiconducting $SrMnO_3$ by solid state reaction route. Ceramic samples of 30 & 40 wt% CuO with above parent matrix ceramics were prepared. From the XRD results it confirms the formation of perfect composites with semiconducting CuO as a secondary phase. Surface morphology study from SEM confirms the presence of both types of grains. Dielectric studies were carried out at four selected frequencies (1 kHz, 10 kHz, 100 kHz, 1 MHz). The result has shown the extraordinarily improved dielectric constant. Maxwell-Wagner polarization (interfacial polarization) was made responsible for the improved result. Dielectric loss also increased by a considerable manner.

List Of Figures

List of table

DEDICATED
TO
MY PARENTS

CHAPTER 1

1.1 Introduction

The electronic industries are now largely focusing on the miniaturization of the devices with uncompromised efficiency. This targets materials having large static dielectric constant that can reduce the volume of the capacitor like elements. Ferroelectric materials are seen to posses large dielectric constant. The Relaxor ferroelectrics have been experienced with relative permittivity value touching 10^4 figures. But this large figure is over dependence on the temperature i.e. after Curie temperature, it suddenly reduces to a minimum which restricts its reliability. Therefore the researchers have swift their interest in searching novel non ferroelectric materials having large dielectric constant in a wide temperature range. $CaCu_3Ti_4O_{12}$ (CCTO) has been emerged as such interesting material having relative permittivity 10^4 figure in a wide temperature range. Li and Ti doped NiO (LTNO) is also showing the same behavior. There are two other groups of monolithic phase ceramics with giant dielectric constant, $AFe1/2B1/2O_3$ where, A=Ba, Sr and B= Nb, Ta. The dispersed metal particle Ni into BaTiO3 ceramic matrix has enhanced the highest dielectric constant of 80,000 which was explained by the theory of percolation.

Polycrystalline CuO also found out as a giant dielectric material exhibiting a striking dielectric constant of 2 x 104 values. The micro traces of Cu^{+3} are found to be responsible for this unusual behavior as reported by *sudipta et al*. CuO is mainly known as a low melting flux former vastly used for densification purpose in liquid phase sintering process.

1.2 Literature survey

Colossal magneto resistancemanganite are known for the unusually large effect an external magnetic field has on their ability to transport electricity and heat. While many of these effects were known more than 50 years ago (van Santen and Junkers, 1950), an appreciation of the size of these effects is a more recent development (Jin, Tiefel *et al.*, 1994). A sensitivity of this magnitude is not observed in any bulk metallic system where, mostly at low temperatures, magnetoresistance arises from a field dependent electronic mean free path. This effect is measurable only in those metals that have a large mean free path in zero fields, i.e., very clean systems, where the magnetic field reduces the mean free path by inducing the electrons to move

in orbits. Even then, the resistivity change is usually limited to a few percent in practical magnetic fields.

Giant-magneto résistance multilayer metallic films show a relatively large sensitivity to magnetic fields. The mechanism in these films is largely due to what is known asthe spin-valve effect between spin polarized metals. If an electron in a regular metal is forced to move across a spin-polarized metallic layer (or between spin-polarized layers) it will suffer spin-dependent scattering. If the electron was initially polarized parallel to that of the layer the scattering rate is relatively low; if originally polarized antiparallel to that of the layer the scattering is high. (The reverse is also possible.) The effect of an external field is to increase the ratio of the former events, reducing the latter, by aligning the polarization of the magnetic layer along the direction of the external field. This effect is a few tens of percent, and has the very important advantage of not being limited to low temperatures. Spin-valve devices have been used in the magnetic storage industry for several years now, in the form of magneto resistive read heads. While the physical mechanism that produces the magneto resistance is well understood, the technological challenges involved in the production of small devices of high sensitivity are the bottleneck of an industry ever hungry for smaller-fasterbetter sensors.

$AMnO_3$ (A = Ca,Sr, Ba, La, Pr, Nd, Dy, Ce) compounds are extensively studied because they have interesting electronic, magnetic, and structural properties (1-4).Recently focused on multiferroic behaviour and their properties on thin films. $CaMnO_3$ crystallizes in the $GdFeO_3$-typeperovskite structure (space group Pnma, Z = 4, a = 5.2770 A°,b = 7.4510 A°, c = 5.2643) with corner-sharing MnO6 octahedra. The antiferromagnetic Neel temperature T_N is 125 K.BaMnO3 adopts a 2*H* hexagonal structure (space group*P*63/*mmc*, *Z* = 2, *a* =5.6991 A°,*c*= 4.8148) with face-sharing MnO6 octahedralwhereH stands for a hexagonal system, and a numeral indicates that a number of the layers inthe unit cell. Stoichiometric $BaMnO_3$, oxygen-deficient $BaMnO_{3-\delta}$ adopts different hexagonal/rhombohedra structures with variable ratios of corner-sharing (cubic) and face-sharing (hexagonal) layers.Using a high-pressure, high-temperature (HPHT) method, the 4*H* and 9*R* (*R* means a rhombohedral system) polymorphs of stoichiometric $BaMnO_3$ can be achieved (5-8).

$SrMnO_3$ is a rare example of a compound having both cubic (high-temperature, high pressure) and a hexagonal at (low temperature) Perovskite polymorph(9-11).Stoichiometric

$SrMnO_3$form three polymorphs such as 4*H* and 6*H*hexagonal and cubic (*C*) perovskite. The former is built from corner-sharing MnO6 octahedral only, the latter contains corner-sharing confacial bioctahedral Mn_2O_9 entities along the *c* axis. Both cubic and hexagonal polymorphs are insulators at 0 K but have quite different band gaps (0.3 vs. 1.6 ev). The hexagonal ground state shows antiferromagnetic coupling both within Mn_2O_9 entities and between the Mn ions in the corner-sharing octahedral. The lowest energy cubic configuration found to be *G*-type antiferromagnetic While the bonding interactions involving Sr found to be mainly ionic, there is a significant covalent contribution to the Mn-O bond. This covalency is very important for the stabilization of hexagonal structure compared to the cubic polymorph. Two additional factors which stabilize hexagonal $SrMnO_3$ relative to the cubic polymorph.

i) The Mn atoms in the face-sharing octahedral displaced along the *c* axis by about 0.012 Å from center of the octahedral.

ii)The charge transfer giving lower charges for the oxygen in the face-sharing triangle compared to the corner-sharing oxygen.

The 6*H*-$SrMnO_3$ polymorph crystal structure was refined using synchrotron x-ray powder diffraction data (space group *P*63/*mmc*(no. 194), *Z* = 6, *a* = 5.42892 A° , *c* = 13.4025 A°).(12-14) Magnetic and transport properties of 6*H*-$SrMnO_3$ were investigated using direct current magnetization, specific heat, and resistivity measurements. The AFN temperature *T*N of 6*H*-$SrMnO_3$ is 235 K; this value is close to that of cubic-$SrMnO_3$ (T_N= 240 K) and 4*H*-$SrMnO_3$ (T_N= 280 K). 6*H*-$SrMnO_3$ and 4*H*-$SrMnO_3$ have the same building blocks of face-sharing MnO6 octahedral.

Above the Neel temperature, 4*H*-SrMnO3 shows a broad anomaly in magnetic susceptibility due to short-range AFM interactions between the Mn^{4+}ions in the face-sharing MnO_6octahedra.This high-temperature anomaly was the reason for the erroneouslyreportedT_N= 350 K in the early studies.*C*-$SrMnO_3$ (space group *Pm*–3*m*, *Z* = 1, *a* = 3.8041 A°) adopts a G-type AFM structure below T_N= 230–260 K.The difference in T_N isprobably due to small variations in the oxygen stoichiometry. Oxygen nonstoichiometric $SrMnO_{3-\delta}$ samples have also been extensively investigated in Refs. (15-17). The lattice sites remain in the ideal cubic perovskite positions with Sr in (0,0,0), Mn in (1/2,1/2,1/2) and O in(1/2,1/2,0)While the *A* cations are surrounded by twelve anions in a cubo-octahedral coordination, the *B* cations are surrounded by six anions in octahedral coordination. The O anions are coordinated by two *B*-site

cations and four *A*-site cations. $SrMnO_3$ alternatively takes a hexagonal perovskite-type structure at low temperatures; a 4*H* polytype in which four layers of manganese are stacked along the *c* direction of the cell, where *H* indicates hexagonalsymmetry. The face-sharing octahedral give rise to Mn_2O_9dimmers,Several magnetically ordered structures are in general possible for cubic perovskites depending on the exchange interactions between neighboring *B*-site cation (*B*-O-*B)* interactions within a defined plane intraplane and between planes interplane. Experiments suggest that cubic $SrMnO_3$ takes the *G*-type AF state.

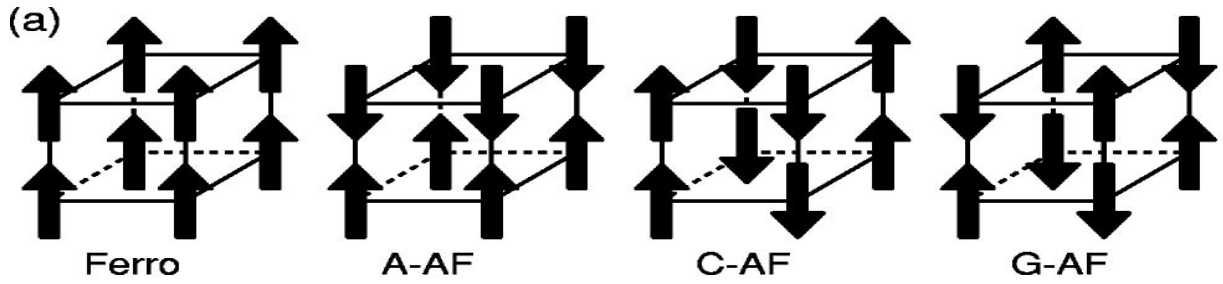

Fig-1 Several magnetically ordered structures

Spin Ordering:

Interactions with neighboring atoms make the spin of electrons align in a particular fashion. We know that Ferromagnetism results when the spins are arranged parallel to one another and antiferromagnetic results when they are anti-parallel to one another.

Antiferromagnetic ordering is three types particularly in preovskite-type oxides..

A-type:

The intra-plane coupling is ferromagnetic while inter-plane coupling is antiferromagnetic.

C-type:

The intra-plane coupling is antiferromagnetic while inter-plane coupling is ferromagnetic.

G-type:

Both intra-plane and inter-plane coupling are antiferromagnetic.

The band-structure calculations suggest that cubic *G*-type antiferromagnetically ordered $SrMnO_3$ is an insulator at 0Kwith a small band gap.The ideal cubic$CaMnO_3$ is found to be *G*-type antiferromagnetically ordered insulator. In a more recent study of $SrMnO_3$ a finite contribution to the electronic density of state in a one spin direction at the Fermi energy was obtained and suggesting half-metallic behavior.

1.3 About $SrTiO_3$

Strontium titanate is an oxide of strontium and titanium with the chemical formula$SrTiO_3$. At room temperature, it is a Centro symmetric paraelectricmaterial with a perovskite structure in which Ti^{4+} ions are six fold coordinated by O^{2-} ions, whereas each of the Sr^{2+} ions is surrounded by four TiO_6 octahedral. Therefore, each Sr^{2+} ion is coordinated by 12 O^{2-} ions. Within the TiO_6octahedral, while a hybridization of the O-2p states with the Ti-3d states leads to a pronounced covalent bonding, Sr^{2+} and O^{2-} ions exhibit ionic bonding character. Hence, $SrTiO_3$ has mixed ionic-covalent bonding properties. This nature of chemical bonding leads to a unique structure, which make it a model electronic material. At low temperatures it approaches a ferroelectric phase transition with a very large dielectric constant ~10^4 but remains Para electric down to the lowest temperatures measured as a result of quantum fluctuations, making it a quantum Para electric. SrTiO3 undergoes a structural phase transition from cubic (*a* = 3.905 A°) to tetragonal (*c*/*a* = 1.00056) phase at ~105 K[21].A distortion from cubic to lower symmetries also can occurs if a foreigner cation/dopant is introduced in the lattice (e.g. ion implantation). Distortions are depends to three main effects: size effects, deviations from the ideal composition and the Jahn- Teller effect.

1.4 About CuO

Transition-metal oxides exhibit various phenomena such as high-temperature superconductivity and colossalmagneto résistance. Recent extensive studies gives another potential of transition-metal oxides as multiferroics in which magnetism and Ferro electricity coexist and are coupled (18-20).The monoclinic crystal structure of CuO comprises zigzag Cu-O chains.CuO contains two successive magnetic transitions at T_{N1}=213 K and T_{N2}=230 K.The simultaneous presence of electric and magnetic ordering, known as multiferroic behavior, is particularly intriguing when the ferroelectric polarization is triggered by a specific magnetic order, and was observed for the first time by Kimura andco-workers in $TbMnO_3$. Since then, several so-called type-II multiferroics have been discovered in which magnetic order causes ferroelectric order.The very recent discovery that cupric oxide (CuO) is a type-II multiferroic with a high antiferromagnetic (AF) transition temperature T_N of 230 K changed this situation drastically and opened a possible route to room-temperature multiferroicity.ApeculiarFeature of CuO is that its type-II behavior is only present at finite temperatures, between T 210K and T 230 K, disappearing above and below.

CHAPTER 2

THESIS OBJECTIVE

- To study the effect of CuO on dielectric properties by making its composite with materials having low dielectric constant of formula (1-x)$SrTiO_3$/$SrMnO_3$-xCuO
- To characterize the synthesized material like XRD for phase formation, SEM for surface morphology and Electrical study for dielectric constant and tangent loss

CHAPTER 3

3.1 Synthesis Methods

3.1.1 Ball milling:

There are two types of ball milling. One is low energy ball milling and another is high energy ball milling. In low energy ball milling rotational kinetic energy is less but in high energy ball milling rotational kinetic energy is high. I have ball milled in high energy. With the help of ball milling materials are grinded into fine powders. In this process high energies are released due to difference in speeds between zirconia balls and the grinding jar.. With the help of acetone we can remove the impurity from the grinding jar.

3.1.2 Calcination:

In calcination solid phase reaction takes place among the constituents by interdiffusion of their ions giving the desired product. In this thermal process thermal decomposition, phase transition takes place. It occurs above transition temperature for phase transition. Higher the calcination temperature the homogeneity and density of final ceramic product. Proper calcination temperature is required to obtain better electrical and mechanical properties. In calcination CO_2 is vaporized.

3.1.3 Sintering:

When thermal energy is applied to a ceramic powder compact at that time the compact is densified and average grain size increases. This process is called as sintering and the basic phenomena ocuurs in this process is densification and grain growth. With increase in sintering temperature the densities of ferroelectric ceramics increases.

3.1.4 Binder addition:

Binders (PVA) used in small concentration serve to provide bridges between the particles.

3.2 Characterization Methods

3.2.1 X-ray Diffraction:

X-rays are electromagnetic wave in the spectrum between gamma-rays and the ultraviolet of wavelength about 1^{o}A. The energetic x rays can penetrate deep into the materials and provide information about the bulk structure. XRD is an important technique used to determine (a) crystal structure (b) crystallite size (3) unit cell lattice parameters and Bravais lattice symmetry, (d) Texture/orientation in polycrystalline or powdered solid samples,(e) phase composition of a sample etc. For phase identification calcined powders and sintered pellets are examined by X-ray diffraction.

Diffraction can occur only when Bragg's law is satisfied i.enλ=2dsinϴ and corresponding XRD peaks are obtained.

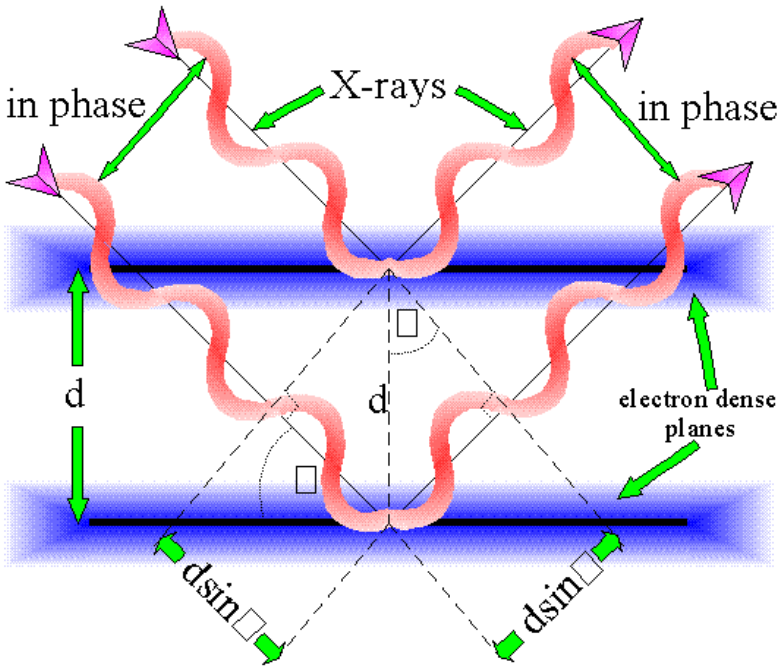

Fig-2 The Diffraction of X-rays by a family of planes

Braggs law can be used to obtain the lattice spacing of a particular cubic system through the following relation.

d =a/ $\sqrt{h^2 + k^2 + l^2}$

Where'a' is the lattice spacing of the cubic crystal and h, k, l are the Miller indices of the Bragg plane.

3.2.2 SEM:

Scanning electron microscope is used to for measuring specimen topography at high magnification. It is a type of electron microscope that images the sample surface by scanning it with a high energy beam of electrons in raster scan process. SEM is a used for identifying the microstructure of ferroelectric ceramics.

Scanning process:

A stream of electrons formed at the electron surface and accelerated towards the specimen using positive electric potential. The stream of electron is confined and focused using metal apertures and magnetic lenses into a thin focused monochromatic beam. The beam is focused onto the sample using a magnetic lens. Interactions occur inside the irradiated sample affects the electron beam.

3.2.3 Dielectric:

A dielectric is an electrical insulator which can be polarized by the action of an applied electric field. When a dielectric is placed in an electric field, electric charge do not flow through the material, as in a conductor, but only slightly shift from their average equilibrium position causing dielectric polarization: positive charges are displaced along the field and negative charges shift in the opposite direction.

.Itisimportanttoexplainvariousphenomenonsinelectronics, optics, andsolid-statephysics.Adielectricmaterialisasubstancethat isa poorconductorofelectricity, butan efficientsupporterofelectrostaticfields.Thispropertyisusefulincapacitors,especiallyatradiofrequencies. Dielectric materialsarealso used inthe constructionofradio-frequencytransmissionlines.

3.3 Experimental Work

The $SrTiO_3$ ceramic was prepared by solid state route method (Fig-3.2) by taking raw materials such as (i) Strontium carbonate ($SrCO_3$) (ii) Titanium dioxide (TiO_2).After the mixing of these two raw materials ball milled for 24 hrs with the help of Zirconia balls and taking acetone as a medium. With the help of acetone we can remove impurity from the grinding jar.Calcination has been done at 1250^0c for 12 hrs. Then the calcined powders are mixed with polyvinyl alcohol for compactness of the powders. After the calcination, sintering was done at 1000^0c for 5 hrs. Then the sintered pellets are characterized like XRD, SEM and DIELECTRIC study.

The $SrMnO_3$ ceramic was prepared by solid state route method (Fig-3) by taking raw materials such as (i) Strontium carbonate ($SrCO_3$) (ii) Titanium dioxide (MnO_2).After the mixing of these two raw materials ball milled for 24 hrs with the help of Zirconia balls and taking acetone as a medium. With the help of acetone we can remove impurity from the grinding jar.Calcination has been done at 1000^0c for 10 hrs. Then the calcined powders are mixed with polyvinyl alcohol for compactness of the powders. After the calcination, sintering was done at 1200^0c for 6 hrs. Then the sintered pellets are characterized like XRD, SEM and DIELECTRIC study.

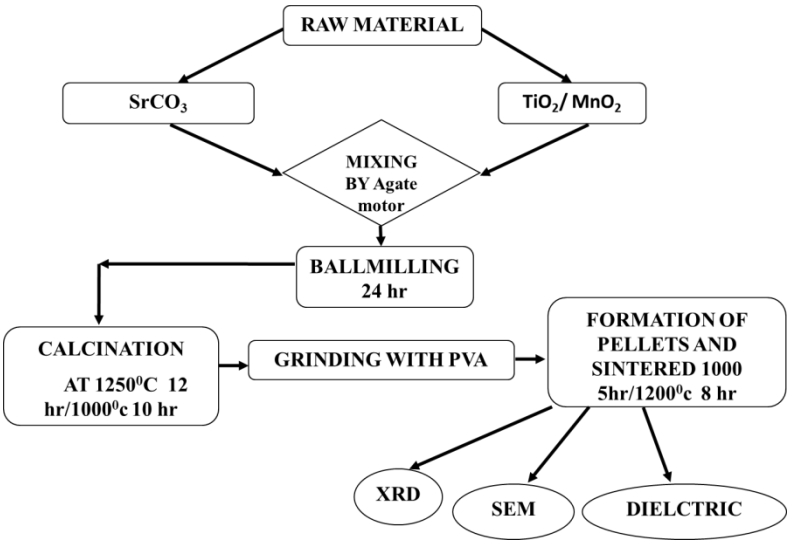

Fig-3 Synthesis method of parent $SrTiO_3$ and parent $SrMnO_3$

For the synthesis of (1-x)$SrTiO_3$-xCuO ceramic composite as wt% of x= 0.3,0.4first used to ball mill for mixing and grinded the mixing powder into fine powder (Fig-4). The prepared powder

was then kept into the programmablefurnace for calcination at the temperature 1100^{o}C of 8hrs for phase formation and removal of a volatile fraction. For making pellets we have to use binder i.e polyvinyl alcohol solution with powder and to make pellets we have to applying around 5 ton pressure for 3 minutes. The prepared pellets sintered at 1200^{o}Cof 6hrs. To knowthe phase formation of prepare sample, XRD analysis technique used and the SEM for surface morphology of (1-x)$SrTiO_3$-xCuO ceramic composite and finally the electrical properties i.e dielectric constant is measured.

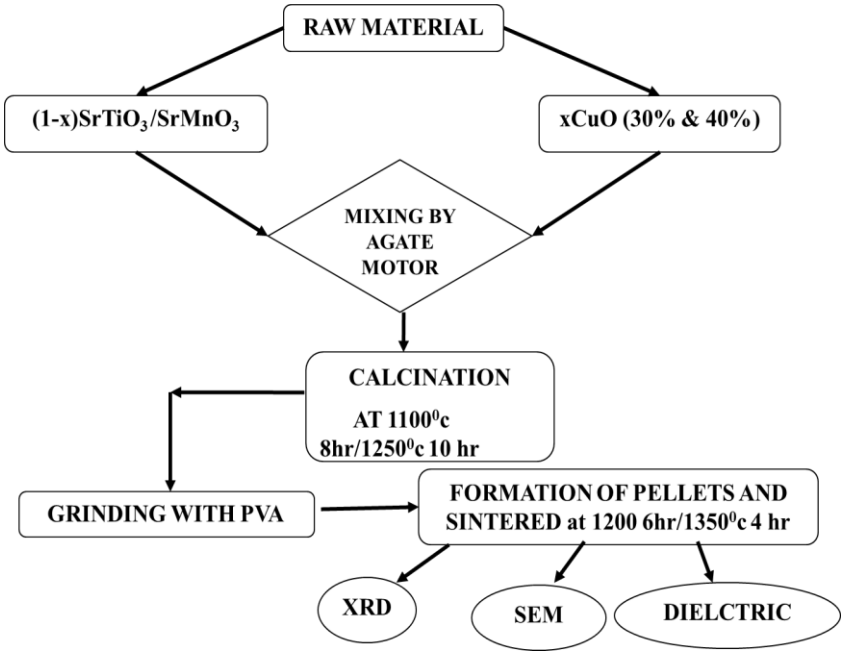

Fig-4 Synthesis method of (1-x)$SrTiO_3$/$SrMnO_3$- xCuO

For the synthesis of (1-x) $SrMnO_3$-xCuO ceramic composite as wt% of x= 0.3,0.4 first used to ball mill for mixing and grinded the mixing powder into fine powder. The prepared powder was then kept into the programmable furnace for calcination at the temperature 1250^{o}C of 10hrs for phase formation and removal of a volatile fraction. For making pellets we have to use binder i.e polyvinyl alcohol solution with powder and to make pellets we have to applying around 5 ton pressure for 3 minutes. The prepared pellets sintered at 1350^{o}Cof 4hrs. To knowthe phase formation of prepare sample, XRD analysis technique used and the SEM for surface morphology of (1-x)$SrMnO_3$-xCuO ceramic composite and finally the electrical properties i.e dielectric constant is measured.

CHAPTER 4

Result and Discussion

4.1 XRD Analysis

From the XRD result it confirms the presence of CuO as a secondary phase in the matrix of both $SrTiO_3$ and $SrMnO_3$. This confirms the formation of desired composite. The main peaks in both cases are observed that the peaks are shifted towards lower diffraction angle.

The main reason for the peak shifts are i) Lattice parameter changes ii) Presence of residual stress and iii) Defect concentration. The Cu^{2+} has the ionic radii very close to Ti^{4+} and Mn^{4+}so there is a possibility to substitute these Cu^{2+} ion into Ti^{4+} and Mn^{4+}. So vacancy is created, that vacancy is the reason to shift the peak.

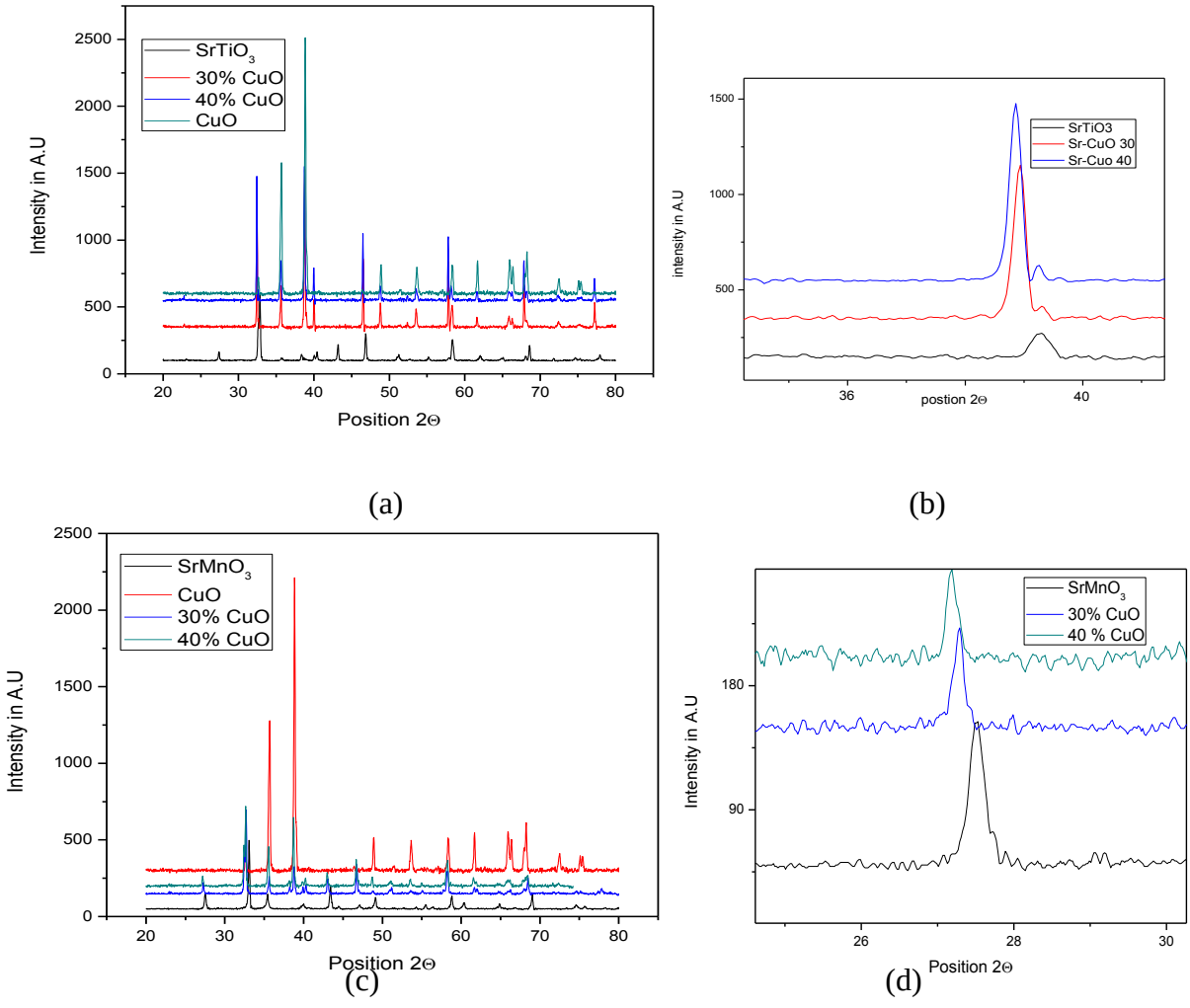

Fig-6 Shows the XRD Pattern of Parent, Composites and their corresponding peak shft (a) SrTiO3,Cuo and wt% Cuo Composites (b) Peak shift of SrTiO3with wt% Cuo Composites (c) SrMnO3,Cuo and wt% Cuo Composites (d) Peak shift of SrMnO3with wt% Cuo Composites

When the XRD result analyzed carefully it is found that the peak shifts towards lower diffraction angle signifies increase in lattice parameter i.e increase in unit cell volume.

4.2 SEMAnalysis

From SEM images of both the composites the minute particles are the CuO grains which confirms the XRD results of forming the composites.

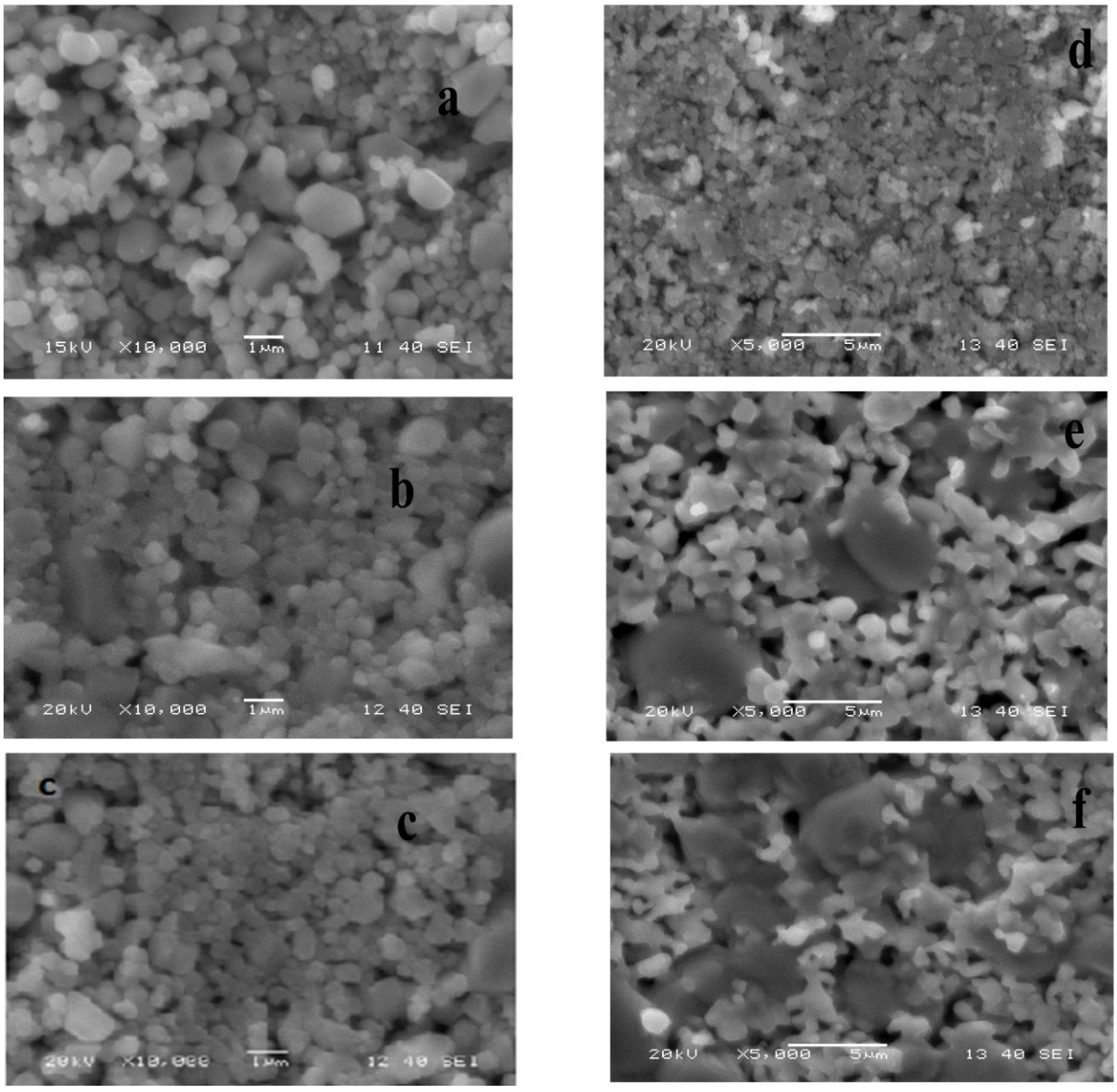

Fig-7 Shows SEM images(a) $SrTiO_3$(b) 30% CuO with $SrTiO_3$ (c) 40%CuO with $SrTiO_3$ (d) $SrMnO_3$ (e) 30% CuOwith $SrMnO_3$(f) 40% CuO with$SrMnO_3$

4.3 Dielectric Result

The dielectric constant against temperature at four selected frequencies (1kHZ, 10kHZ,100kHZ,1MHZ) were taken with the help of an LCR meter. It observed that, the dielectric constant is very low for both $SrTiO_3$and $SrMnO_3$.The dielectric loss (tanδ) for $SrTiO_3$ is significantly low as it is a good insulator and Para electric at room temperature. But in case of $SrMnO_3$ the dielectric loss rises to a high value after certain temperature due to its semiconducting nature. Dielectric study for both the materials were done with CuO as a secondary precursor with 30 and 40 wt%of parent material.

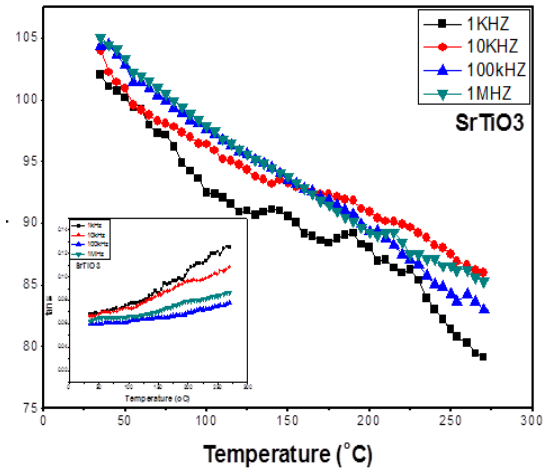

(a)

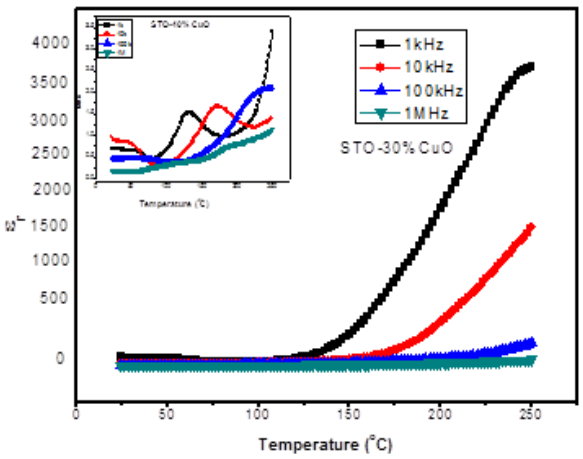

(b)

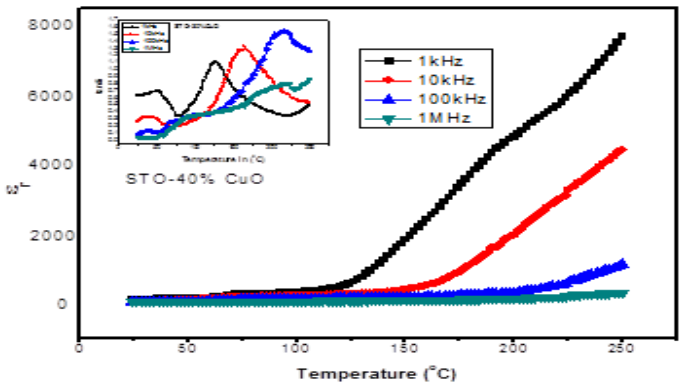

(c)

Fig-8 Dielectric Constant and tangent Loss of (a) $SrTiO_3$ (b) 30% CuO (c) 40% CuO

Table-1

Parent and composition of $SrTiO_3$	ε_r at room temp. at 1kHz	ε_r at 250 °C at 1 KHz	Tanδ at room temp. at 1kHz	Tanδ at 250 °C temp. at 1kHz
$SrTiO_3$	103	79	0.09	1.025
$SrTiO_3$+30% CuO	157	3838	0.60	0.50
$SrTiO_3$+40% CuO	291	7851	0.66	3.38

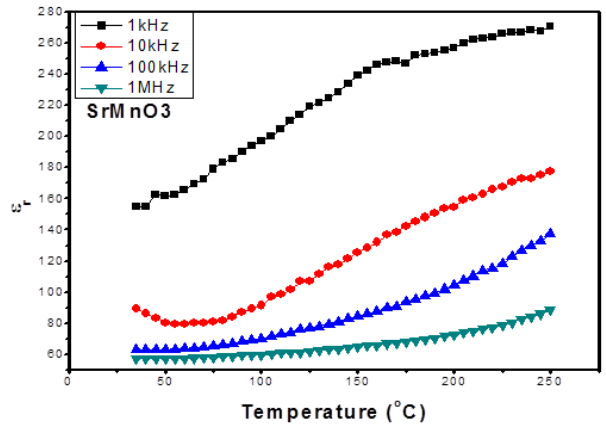

(a)

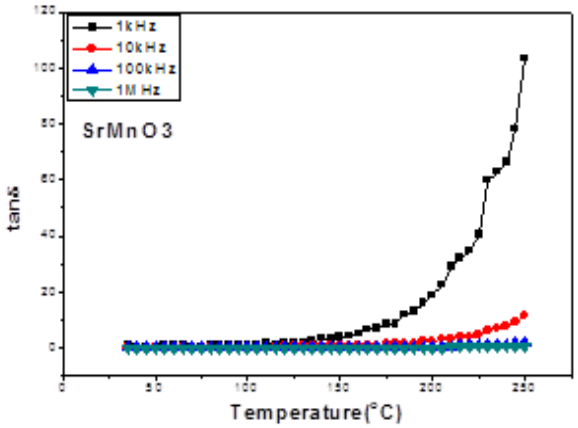

(b)

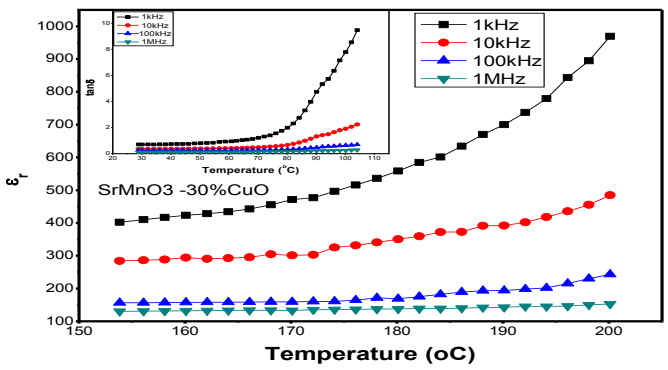

(c)

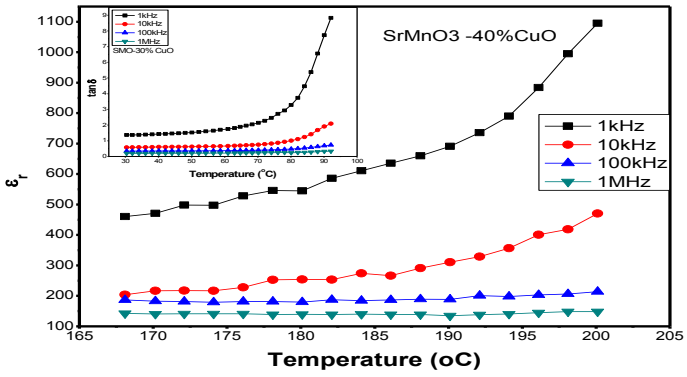

(d)

Fig-9 Dielectric Constant and tangent Loss of (a) $SrMnO_3$ (b) tanδ of $SrMnO_3$ (c) with 30% CuO (d) with 40% CuO

Table-2

Parent and composition of $SrMnO_3$	Ɛr at room temp.at 1kHz	Ɛrat 200 ^oC at 1 KHz
$SrMnO_3$	**151**	**272**
$SrMnO_3$+30% CuO	**400**	**969**
$SrMnO_3$+40% CuO	**450**	**1045**

From the Fig-8 it was found that the dielectric constants ($Ɛ_r$) vs temperature graph of $SrTiO_3$ of different frequencies behaves very interestingly. The $Ɛ_r$ value touches around 4000 at 1kHZ frequency for 30 wt% of CuO and for 40 wt% of CuO, $Ɛ_r$ value approaches 9800 value. But the dielectric loss also increased with a significant value with well observed relaxation peaks. The relaxation is the phenomenon when energy of different types of stress are released. When they are in stress mode at that time dielectric constant is high. From the Fig-9 the dielectric constants ($Ɛ_r$) vs temperature graph of $SrMnO_3$ of different frequencies was observed. It was found that the $Ɛ_r$ value touches around 1000 at 1kHZ frequency for 30 wt% of CuO and for 40 wt% of CuO $Ɛ_r$ value approaches 1100 value. It is also observed that the dielectric loss increases rapidly to a high value for both parent and CuO-$SrMnO_3$ composites.

CHAPTER 5

CONCLUSION

For all composites of (1-x)$SrTiO_3$-xCuO and (1-x) $SrMnO_3$-xCuO with 30% and 40% of CuO the XRD peaks are shifts towards lower diffracting angle which shows the increasing of lattice parameter. The SEM results of (1-x)$SrTiO_3$-xCuO and (1-x) $SrMnO_3$-xCuO with 30% and 40% of CuO shows the grains are uniformly distributed and the presence of extra copper phase increases with increasing % of copper. From dielectric results of (1-x)$SrTiO_3$-xCuO and (1-x) $SrMnO_3$-xCuO shows increasing of dielectric constant and also the tangent loss.

REFERENCES

[1] J. H. Lee and K. M. Rabe, Phys. Rev. Lett. 104, 207204(2010).

[2] S. Smadici, P. Abbamonte, A. Bhattacharya, X. F. Zhai, B. Jiang, A. Rusydi, J. N. Eckstein, S. D. Bader, and J. M. Zuo, Phys. Rev.Lett. 99, 196404 (2007).

[3] I. D. Fawcett, J. E. Sunstrom, M. Greenblatt, M. Croft, and K. V.Ramanujachary, Chem. Mater. 10, 3643 (1998).

[4] E. J. Cussen and P. D. Battle, Chem. Mater. 12, 831(2000).

[5] A. N. Christensen and G. Ollivier, J. Solid State Chem. 4, 131

[6] J. J. Adkin and M. A. Hayward, Chem. Mater. 19, 755(2007).

[7] J. J. Adkin and M. A. Hayward, J. Solid State Chem. 179, 70(2006).

[8] B. L. Chamberland, A. W. Sleight, and J. F. Weiher, J. Solid StateChem. 1, 506 (1970).

[9] Y. Syono, S. I. Akimoto, and K. Kohn, J. Phys. Soc. Jpn. 26, 993(1969).

[10] K. Kuroda, N. Ishizawa, N. Mizutani, and M. Kato, J. Solid State Chem. 38, 297 (1981).

[11] P. D. Battle, T. C. Gibb, and C. W. Jones, J. Solid State Chem. 74,60 (1988)

[12] M. Imada, A. Fujimori, and Y. Tokura, Rev. Mod. Phys. 70,1039_1998_.

[13] N. A. Hill, J. Phys. Chem. B 104, 6694 _2000_.

[14] M. Fiebig, J. Phys. D 38, R123 _2005_.

[15] D. I. Khomskii, J. Magn. Magn.Mater.306, 1 _2006_.

[16] W. Eerenstein, N. D. Mathur, and J. F. Scott, Nature _London_442, 759 _2006_.

[17] S.-W. Cheong and M. V. Mostovoy, Nat. Mater.6, 13 _2007_.

[18] J. B. Forsyth et al., J. Phys. C 21, 2917 (1988).

[19] X. Rocquefelteet al., J. Phys. Condense. Matter 22, 045502(2010).

[20] A. Filippetti and V. Fiorentini, Phys. Rev. Lett. 95, 086405(2005).

[21] J. Ghijsenet al., Phys. Rev. B 38, 11322 (1988).

[22] Introduction to solid state physics by Charles kittle, Willey edition

[23] G. K. Williamson and W. H. Hall, Acta Metall. 1, 22 (1953).

[24](van Santen and Jonker, 1950)